Transcriptome analyses of β-thalassemia -28 (A>G) mutation using isogenic cell models generated by CRISPR/Cas9 and asymmetric single-stranded oligodeoxynucleotides (assODN)

Authors:

Jing Li[1, 2, 3*], Ziheng Zhou[2, 3*], Hai-Xi Sun[2, 3, 5], Wenjie Ouyang[2, 3], Guoyi Dong[2, 3], Tianbin Liu[2, 3], Lei Ge[2, 3], Xiuqing Zhang[2, 3, 6#], Chao Liu[2, 3#] & Ying Gu[2, 3, 4#]

AFFILIATION:

[1] BGI Education Center, University of Chinese Academy of Sciences, Shenzhen 518083, China
[2] BGI-Shenzhen, Shenzhen 518083, China
[3] China National GeneBank, BGI-Shenzhen, Shenzhen 518120, China
[4]Guangdong Provincial Key Laboratory of Genome Read and Write, BGI-Shenzhen, Shenzhen, 518120, China
[5] Institute for Stem cell and Regeneration, Chinese Academy of Sciences, Beijing, 100101, P.R.China
[6]Guangdong Provincial Key Laboratory of Human Disease Genomics, Shenzhen Key Laboratory of Genomics, BGI-Shenzhen, Shenzhen 518083, China
[#]Corresponding authors: guying@cngb.org; liuchao4@cngb.org; zhangxiuqing@genomics.cn

*These authors contributed equally to this work

Abstract

β-thalassemia, caused by mutations in the human hemoglobin (*HBB*) gene, is one of the most common genetic diseases in the world. *HBB* −28 (A>G) mutation is one of the five most common mutations in China patients with β-thalassemia. However, few studies have been conducted to understand how this mutation affects the expression of pathogenesis related genes including globin genes due to limited homologous clinical materials. Therefore, we first developed an efficient technique using CRISPR/Cas9 combined with asymmetric single-stranded oligodeoxynucleotides (assODN) to generate a K562 cell model of *HBB* -28 (A>G) named $K562^{-28\ (A>G)}$. Then, we systematically analyzed the differences between $K562^{-28\ (A>G)}$ and K562 at the transcriptome level by high-throughput RNA-seq pre- and post-erythrogenic

differentiation. We found that *HBB* -28 (A>G) mutation not only disturbed the transcription of *HBB* but also decreased the expression of *HBG*, which may further aggravate the thalassemia phenotype and partially explain the severer clinical outcome of β-thalassemia patients with *HBB* -28 (A>G) mutation. Moreover, we found K562$^{-28\ (A>G)}$ cell line is more sensitive to hypoxia and showed a defective erythrogenic program compared with K562 before differentiation. In agreement, p38MAPK and ERK pathway are hyperactivated in K562$^{-28\ (A>G)}$ after differentiation. Importantly, all above mentioned abnormalities in K562$^{-28\ (A>G)}$ were reversed after correction of this mutation with CRISPR/Cas and assODN, confirming the specificity of these phenotypes. Overall, this is the first time to analyze the effects of the *HBB* -28 (A>G) mutation at whole-transcriptome level based on isogenic cell lines, providing a landscape for further investigation of the mechanism of β-thalassemia with *HBB* -28 (A>G) mutation.

Keywords

beta-thalassemia, *HBB* (−28 A>G), isogenic cells, K562, CRISPR/Cas9, ssODN, RNA-Seq.

Background

Beta-thalassemia is one of most common autosomal recessive blood diseases spread worldwide , caused by either point mutations or deletions in the β-globin (*HBB*) gene[1, 2]. Approximately 80 to 90 million people carried β thalassemia , and about 300,000 children with severe thalassemia are born every year[3-5].Mutations or deletions of β-globin genes result in the reduction of hemoglobin β chain (β-globin), deformation of hemoglobin tetramer and subsequent lysis of erythrocytes, finally causing oxygen shortage, bone deformity, organ dysfunction and even organ failure in many parts of the human body[6, 7]. As for the thalassemia major patients, life-long blood

transfusion and iron chelation treatments are required for survival, but often accompanied by numerous complications, including arrhythmia, congestive heart failure, hypothyroidism, hypoparathyroidism, hypogonadism, diabetes, osteoporosis, liver cirrhosis and recurrent infections. Thus, thalassemia has threatened millions of people's lives for decades and is still a major public health issue[8, 9].

β-thalassemia mutations are prevalent in Southern part of China and Southeast Asia, and *HBB* −28 (A>G) mutation is one of the five most common HBB mutations carried by β-thalassemia patients in China[7, 10]. In *HBB* −28 (A>G) mutation, adenine (A) base located at 28 base pairs upstream from the cap site is mutated to guanine (G), disrupting the binding of transcription factor of ATA box and decreasing the RNA expression of *HBB*[11]. Patients with homozygous or compound heterozygous −28 (A>G) mutation may develop severe anemia or intermedia anemia[6, 11]. Although the description of severe thalassemia has been first published over 90 years ago and a considerable amount work has been reported to refine the understanding of the pathophysiology of thalassemia syndromes in the past 50 years, the cellular and molecular basis of this group of diseases are still not thoroughly investigated [12]. In particular, few studies have been conducted on *HBB* −28 (A>G) mutation to understand how this mutation affects gene expression at transcriptome level, although correcting the *HBB* −28 (A>G) mutation with base editing (BE) system has also been reported in human iPS cells and reconstituted embryos [7].Without full understanding of the defects at molecular level, especially in the short and long run, it will be difficult to comprehensively evaluate the rescue effect after changing the mutation back. In a recent study, high-throughput RNA-sequencing has been used to compare control samples with patient samples carrying a novel *HBB* mutation (*HBB*: c.51C>T). It shows that hemopoiesis, heme biosynthesis, response to oxidative stress and other cellular activities pathway were directly or

indirectly enriched by differentially expressed genes related to β-thalassemia [13], suggesting genome-wide RNA-seq analysis is a useful approach to understand the mechanism of β-thalassemia with different mutations. However, control samples in this study are allogenic, and different genetic backgrounds and mixture of short and longterm effect would prevent deep understanding of effect of each mutation.

In order to explore the specific impact of *HBB* -28 (A>G) mutation on erythroid differentiation and how it affects genome-wide gene expression without confounding factors, such as comparison of allogenic samples, we used CRISPR/Cas9 gene-editing system combined with asymmetric single-stranded oligodeoxynucleotides (assODN) to generate the disease model of isogenic K562 cell lines [14, 15], and then conducted transcriptome analysis by high-throughput RNA-sequencing. The mutant cell line was derived from immortalized K562 and named as $K562^{-28\ (A>G)}$, showing no detectable *HBB* gene expression and enabling comparative studies in the same genome background. We found that *HBB* was prevented from transcriptional expression, and GO and KEGG analysis revealed that $K562^{-28\ (A>G)}$ cell line is more sensitivity to hypoxia and present a defective erythrogenic program when compared with wild type K562 before erythroid differentiation. In agreement, p38MAPK and ERK pathway are hyperactivated in $K562^{-28\ (A>G)}$ after differentiation. Interestingly, *HGB* showed a lower rate of induction in $K562^{-28\ (A>G)}$ when compared with wild type K562 after erythroid differentiation. Taken together, our study is the first time to analyze the effects of the *HBB* -28 (A>G) mutation at whole-transcriptome level based on isogenic cell lines. The unraveled molecular biomarkers and signaling pathways that affected in $K562^{-28\ (A>G)}$ cell line may be further investigated as therapeutic targets to improve the quality of life for those β-thalassemia patients in future studies.

Results

Generation of *HBB*−28 (A>G) mutant cell line by CRISPR/Cas9 and asymmetric single-stranded oligodeoxynucleotides

To study how *HBB* -28 (A>G) mutation affects gene expression at the genome-wide level, isogenic human cell line carrying this mutation was generated. The diagram of generating mutant cell line was shown, including transfection, CRISPR/Cas editing, single cell sorting, cell characterization and expansion (Fig. 1A). As previous studies demonstrated that using single-strand oligodeoxynucleotides (ssODNs) [16] or asymmetric double-strand DNA [17] as repair template resulted in higher efficiency of accurate replacement of target sequences through homology directed repair (HDR), we developed a new technology to combine CRISPR/Cas with asymmetric ssODNs (assODNs). To generate *HBB* -28 (G>A) mutation, sgRNA mediating DNA cleavage 3bp aside from the -28 mutation site and assODN with 36bp on the PAM-distal side and 91bp on PAM-proximal side of the cutting site were used (Fig. 1B). K562, a human erythroleukemia line that resembles undifferentiated erythrocytes, was transduced with these Cas/sgRNA and assODNs. As expected，we identified one cell line with homozygous mutation of *HBB* -28 (A>G) by Sanger sequencing and named it as K562$^{-28\ (A>G)}$ (Fig. 1C). In order to reconfirm the functional mutation of *HBB* -28(A>G), we used qPCR and ELISA to detect the expression of *HBB* mRNA and HBB protein respectively. In agreement with the sequencing result, the expression of *HBB* mRNA and HBB protein was undetectable in K562$^{-28\ (A>G)}$ cell line. In contrast, wild-type K562 showed a considerable expression of *HBB* mRNA and HBB protein even without erythroid differentiation (Fig. 1D and 1E). These results suggested that the mutant cell line of *HBB* -28(A>G) was successfully generated, in which the expression of *HBB* was eliminated.

Transcriptome analysis of K562$^{-28\ (A>G)}$ and K562 before erythrogenic differentiation

Many K562$^{-28\ (A>G)}$ cells appear to have irregular morphology and spontaneous cell death compared to the wt counterpart, suggesting loss of HBB expression by -28(A>G) mutation may compromise cell viability in normal culture condition (supplementary Fig.1). To understand how the mutation affects molecular functions of cells at transcriptional level, we conducted RNA-seq to analyze the transcriptome differences between the isogenic cell line of K562$^{-28\ (A>G)}$ and its control K562. Pairwise Pearson correlation analysis revealed high similarity between replicates from K562$^{-28\ (A>G)}$ and K562 cells, indicating high reproducibility of our data (Fig. 2A). Overall, the gene expression levels between K562$^{-28\ (A>G)}$ and wt cell are similar transcriptome-wide, suggesting that the mutation may affect (Fig. 2B). We conducted analysis of differentially expressed genes (DEG) and found 120 and 524 genes were consistently upregulated and downregulated in K562$^{-28\ (A>G)}$ compared to K562 (Figure 2C). To further explore the affected underlying biological functions, we conducted GO term, KEGG and Reactome analysis using those DEGs and found pathways of (cellular) response to hypoxia and response to (decreased) oxygen level were upregulated in K562$^{-28\ (A>G)}$ mutant cell line (Figure 2D). In consistent, hypoxia related genes such as *HMOX1, BMP7, GATA6, ESAM, RYR2* were upregulated in K562$^{-28\ (A>G)}$ (Figure 2C). Interestingly, PI3K-Akt signaling pathway that is important for erythrocyte differentiation [18], was downregulated in K562$^{-28\ (A>G)}$ (Fig. 2D). To further explore the core regulators, we performed interaction assay to predict transcription factors (TFs) that target upregulated genes in K562$^{-28\ (A>G)}$. In agreement with previous results, we observed *GATA* family, *HOXD10* and *SPIC*, which are well-known regulators of erythroid differentiation and hypoxia [ref]，were the core regulators for upregulated genes in K562$^{-28\ (A>G)}$ (Fig. 2E). The

177 regulators and their corresponsive target genes were listed and genes related
178 to hypoxia response were labelled in red (Fig. 2F). Taken together, these data
179 suggested hypoxia response was upregulated in K562$^{-28\ (A>G)}$ and the core
180 regulators were GATA family, HOXD10 and SPIC.
181
182 **Transcriptome analysis of co-regulated genes in K562$^{-28\ (A>G)}$ and K562**
183 **cell lines after erythroid differentiation**
184 In order to investigate the effect of *HBB* −28 (A>G) mutation during erythroid
185 differentiation, we induced erythroid differentiation and then performed
186 genome-wide RNA-Seq in K562 and K562$^{-28\ (A>G)}$ mutant cell line. Pairwise
187 Pearson correlations represented in matrix indicated that the isogenic cell
188 lines showed high similarities up to 90% and the samples were clustered
189 together depending on their differentiation conditions (Fig. 3A). The
190 expression of 1385 genes were consistently upregulated in differentiated
191 K562$^{-28\ (A>G)}$ and K562 when compared to undifferentiated samples (Fig. 3B)
192 and these DEGs were used to conduct the GO term, KEGG and Reactome
193 analysis. Multiple signaling pathways were activated in both K562$^{-28\ (A>G)}$ and
194 K562 (Fig. 3C), including PI3K-Akt, MAPK and ERK pathways that have
195 been reported to be activated during erythroid differentiation [18-21]. In
196 addition, signal pathways such as cell adhesion, pluripotency of stem cells,
197 platelet activation and Notch pathway, were also co-activated in differentiated
198 samples (Fig. 3C), suggesting our induction process was successful in both
199 cell lines. *HBB* belongs to globin gene family mainly including *HBA* (α-
200 globin), *HBG* (γ-globin) and *HBE* (ε-globin). *HBB, HBG* and *HBE* are β-
201 globin-like and all capable of forming tetramer with α-globin. They are
202 located within a gene cluster on chromosome 11 and their expression are
203 coordinated by the same locus control region (LCR) with other regulatory
204 DNA elements [22]. In β–thalassemia patients, *HBG* may be upregulated to
205 compensate the loss of *HBB*. To study the compensatory gene expression of
206 globin genes in K562$^{-28\ (A>G)}$ after differentiation, the expression of *HBB*, *HBA*

and *HBG* was analyzed by RNA-sequencing in isogenic cell lines of K562$^{-28\ (A>G)}$ and K562. As expected, Integrative Genomics Viewer（IGV）analysis showed that *HBB* expression was induced in K562 but undetectable in K562$^{-28\ (A>G)}$ after differentiation (Fig. 3D). In contrast, expression of other globin genes was induced and detected in K562$^{-28\ (A>G)}$ after differentiation (Fig. 3E). we noticed that fold induction rate of *HBA1, HBA2, HBE1 and HBZ* were similar or slightly increased in K562$^{-28\ (A>G)}$-Dif when compared to those in K562-Dif. However, *HBG* expression in K562$^{-28\ (A>G)}$-Dif was generally lower than K562-Dif (Fig. 3F). The expression of *HBB* and *HBG* before and after differentiation were further confirmed by RT-PCR. In consistent, expression of *HBB* was undetectable in undifferentiated K562$^{-28\ (A>G)}$ and its expression level in K562$^{-28\ (A>G)}$-Dif after differentiation was negligible when compared to K562-Dif control (Fig. 3G). In agreement with RNA-seq results, expression level of *HBG* was increased in both cell lines after differentiation, but induction fold of *HBG* was lower in K562$^{-28\ (A>G)}$ than that in K562 (Fig. 3G and 3H). We further analyzed the expression of key transcription factors that are important for regulation of globin genes during erythrogenic differentiation. KLF1, a positive regulator of *HBG* expression, is downregulated in K562$^{-28\ (A>G)}$. Expression of other positive regulators, including GATA1, BGL3 and NFE2 [19, 23-25], were dramatically upregulated in K562 after differentiation, while those increasement were largely attenuated in K562$^{-28\ (A>G)}$. In contrast, negative regulator BCL11A was upregulated in K562$^{-28\ (A>G)}$ before differentiation (Fig. 3I). Those data suggested the erythrogenic differentiation was overall normal in K562$^{-28\ (A>G)}$, but *HBB* -28 (A>G) mutation may affect the *HBG* expression through a network of transcription factors.

Transcriptome analysis of differentially expressed genes (DEGs) in K562 and K562$^{-28\ (A>G)}$ cell lines after erythroid differentiation

To understand the effect of HBB -28 (A>G) mutation during erythrogenic

differentiation, we identified the DEGs within K562$^{-28\ (A>G)}$-Dif and K562-Dif. The number of upregulated and downregulated DGEs in K562$^{-28\ (A>G)}$ were 158 and 740 respectively (Fig. 4A). With GO term, KEGG and Reactome analysis, we found up-regulated DEGs in K562$^{-28\ (A>G)}$-Dif were enriched in pathways related to stress-response and hematopoiesis disorder, such as regulation of apoptosis process, negative regulation of leukocyte activation, myeloid leukocyte cytokine production, negative regulation of blood coagulation, negative regulation of hemostasis, and negative regulation of hemopoiesis. Meanwhile, down-regulated DEGs in K562$^{-28\ (A>G)}$-Dif were enriched in oxygen related pathways, including oxygen transport, erythrocytes take up carbon dioxide and release oxygen and O2/CO2 exchange in erythrocytes (Fig. 4B). Reactome analysis of critical DEGs and their related KEGG pathways in differentiated K562$^{-28\ (A>G)}$-Dif was shown, and *PDE4D*, *TFPI* and *CA1, AQP1* which were related to hypoxia were found to be critical targets (Figure 4C and Supplementary table 1). Moreover, TF prediction revealed that JAZF1, MSI2, KDM4, HOX and ZNF family were core regulators for upregulated genes in K562$^{-28\ (A>G)}$-Dif (Fig. 4D), while SPIC and GATA family are core regulators for downregulated genes in K562$^{-28\ (A>G)}$-Dif (Fig. 4E). Interestingly, GATA3 was found to be the core regulator for both upregulated and downregulated genes (Fig. 4D and E). Taken together, dysregulated genes and pathways were present in K562$^{-28\ (A>G)}$ after differentiation and transcription factors, such as GATA, HOX and ZNF families, may play important roles as core regulators.

Reversion of observed abnormalities in corrected K562^{-28cor} cell line

As it took weeks for the generation of K562 mutant cells by Crispr/Cas9 and clone selection, it is possible that the diffrerential gene expression is due to secondary effects of the mutation and HBB loss, similar to studies of patient samples (ref). In order to determine the specificity of changed gene expression that attributes to the mutation, we corrected the *HBB* -28 (G>A)

mutation in K562$^{-28\ (A>G)}$ by the same strategy of CRISPR/Cas9 combined with assODN (Fig. 5A and supplementary Fig.2), and named the corrected cell line as K562$^{-28(A>G)cor}$. We analyzed the correlation of RNA-seq data between K562$^{-28(A>G)cor}$, K562 and K562$^{-28\ (A>G)}$ and found expression profile of K562$^{-28(A>G)cor}$ was closer to K562 rather than its precursor K562$^{-28\ (A>G)}$ (Fig. 5B). DEGs of isogenic cell lines were showed in the form of heat map and results indicated that upregulated and downregulated genes in K562$^{-28\ (A>G)}$ were reversed in K562$^{-28(A>G)cor}$ (Fig. 5C). Through analysis of pathway enrichment, PI3K pathway and cell response to oxygen pathway were recovered in K562$^{-28(A>G)cor}$ and the related genes, including *BMP7*, *EGR1* and *KCND2*, were showed in heatmap. The erythroid transcriptional factors such as *GATA1, KLF1* and *BCL11A*, were also recovered in K562$^{-28(A>G)cor}$ (Fig. 5D and E and supplementary Fig. 5A and B). In summary, a large portion of abnormalities observed in K562$^{-28\ (A>G)}$ are reversed in corrected K562$^{-28(A>G)cor}$, suggesting these phenotypes are specifically caused by mutation of *HBB* -28 (A>G).

Discussion

In our study, we successfully generated the cell line K562$^{-28\ (A>G)}$ with *HBB* 28 (A>G) mutation using CRISPR/Cas9 and a 127bp assODN. This disease model of cell line was used to study how *HBB* -28 (A>G) mutation affected the cellular function on transcriptome level pre- and post-erythroid differentiation .

Our results showed *HBB* -28 (A>G) mutation prevented the transcription of *HBB* gene. Analysis of enriched pathways suggested PI3K pathway, as well as JAK-STAT pathway, which play important roles in the erythroid differentiation, were disrupted in K562$^{-28\ (A>G)}$ before erythroid differentiation. The PI3K-Akt signaling pathway is a significant pathway that control many

cellular processes known as cell division, autophagy, survival, and differentiation [ref]. Moreover, the mutation activated the hypoxia pathway in undifferentiated K562$^{-28\ (A>G)}$. Many clinical manifestations observed in β–thalassemia is attributed to the chronic hypoxic environment due to pathologic erythrocyte production, and our data suggest hematopoietic precursors may also subject to oxidative stress before differentiation.

To induce erythroid differentiation, we chose the glutamine-minus medium with sodium butyrate, as hemoglobin synthesis was markedly induced using this condition with a differentiation efficiency of 11%~19% in K562 [26, 27]. Consistent with previous reports, the differentiation efficiency of K562 in our study was nearly 12% (data not shown), indicating that our erythroid differentiation is effective. In agreement, the MAPK and ERK pathway was activated in both K562 and K562$^{-28\ (A>G)}$ (Fig. 2), a finding consistent with observations in previous studies [20, 28]. Interestingly, PI3K-Akt signaling pathway was activated in K562$^{-28\ (A>G)}$ after induction, suggesting the defective PI3K pathway may be caused by lack of activators in undifferentiated K562$^{-28\ (A>G)}$. Other pathways, such as cell adhesion, pluripotency of stem cells, platelet activation and Notch pathway, were also co-activated in differentiated K562 and K562$^{-28\ (A>G)}$ samples, indicating mutation of *HBB* -28 (G>A) didn't block the pathways required for differentiation. Nevertheless, in consistent with data from undifferentiated K562$^{-28\ (A>G)}$, oxygen related pathways were downregulated in differentiated K562$^{-28\ (A>G)}$ (Fig. 4). In both undifferentiated and differentiated conditions, SPIC and GATA families are predicted as core regulators (Fig.2 and Fig.4). The GATA family of transcription factors (GATA1-6) are essential for normal hematopoiesis and a multitude of other developmental processes [19, 29]. *GATA-1* regulates terminal differentiation and function of erythroid which activates or represses erythroid-specific gene, such as β-globin locus-binding protein, and it might regulate the switch of fetal to adult haemoglobin in human [30].

Interestingly, increased expression of *GATA1* was largely attenuated in K562$^{-28\ (A>G)}$ during erythroid differentiation (Fig. 3), which may play a role for dysregulated oxygen related pathways.

As improving the levels of *HBG* in adults could partially reverse the severity of symptoms in sickle disease and β–thalassemia, it is important to understand the coordinated regulation between *HBB* and *HBG* [31-34]. In this study, we noticed that fold induction of *HBG* was decreased in K562$^{-28\ (A>G)}$. *ZBTB7A* and *BCL11A* were two major repressors of *HBG* by directly bound the *HBG* gene promoters [24, 35-37]. Expression of *ZBTB7A* was decreased during differentiation in K562, consistent with increased expression of *HBG*. However, the overall expression level was higher in K562 than that in K562$^{-28\ (A>G)}$, paradoxical with the results of decreased fold induction of *HBG* in mutant cell line. Although expression of *BCL11A* was lower in K562 when compared to 562$^{-28\ (A>G)}$ before differentiation, its expression increased dramatically during differentiation (Figure3I and supplementary Figure5). Collectively, our data suggest the expression of *HBG* was not only regulated by *ZBTB7A* and *BCL11A,* but may also be regulated by GATA proteins that also regulate *HBB*. However, the interaction requires further investigations.

Lastly, we not only used CRISPR/Cas9 to generate mutation but also corrected the mutation with the same strategy (Fig. 5A). On one aspect, reversed abnormalities in corrected cell line confirmed the specificities of these phenotypes. On another aspect, the efficient editing results indicate our gene editing strategy using assODN is powerful and provide means for gene editing treatment of *HBB* mutation with -28(A>G).

In summary, we show isogenic K562$^{-28\ (A>G)}$ cell line generated with CRISPR/Cas and assODN is a valuable model to evaluate the β-thalassemia with homozygous mutation of *HBB* -28 (A>G). It provides us with the first

transcriptome data for mechanistic study on the effects of *HBB* -28 (A>G), and our disease model may also be used to assay the new therapies against β−thalassemia in the future.

Data Availability

The data of our study have been deposited in the CNSA (https://db.cngb.org/cnsa/) of CNGBdb with accession code CNP0000981.

ACKNOWLEDGEMENTS

We would like to thank Yanmei Deng, Jiaying Zhang and Wenwen Yao for helping single cell identification. We thank the Genome Synthesis and Editing Platform of the China National GeneBank for providing support on gene synthesis. We thank BGI colleagues for helping to output the high-quality data. This research was supported by National Natural Science Foundation of China (No.31970816 and 81903159), Guangdong Provincial Key Laboratory of Genome Read and Write（No. 2017B030301011）and Shenzhen Municipal Government of China (No.20170731162715261)

AUTHOR CONTRIBUTIONS

Y.G., C.L. and X.Z conceived and designed the study. J.L performed experiment from L.G, T.L, G.D and Ouyang; Z.Z, and H.S performed bioinformatics analysis; J.L., Z.Z., Y.G and C.L. wrote the manuscript with the inputs from all authors.

Methods

Generation of β-thalassemia with-28 (A/G) cell line and corrected cell line

sgRNA design and construction: two 20-bp sgRNAs were chosen containing the -28 (A/G) site, and the cutting site about 3 bp and 9bp before

the mutation site respectively, the sequence we showed in Figure1B.**T**he guide RNA oligonucleotides were synthesis by BGI and inserted into the gRNA cloning vector pSpCas9(BB)-2A-GFP (PX458) (Add gene 48138) according to the protocol provided by Zhang F's protocol[38].

Design of ss ODN repair templates :The 127-nt asymmetric ss ODN repair templates were designed by overlapped the CRISPR/Cas9 cleavage site with 36 bp on the PAM-distal side, and with a 91-bp extension on the PAM-proximal side of the break[16, 17]（Figure1A and 1B）and were synthesized by BGI. Once the mutation of -28 (A/G) were mutated, the site was blocked and Cas9 could not cut this site again without anything changed. So, it is easy manipulate and seamless on the genome.

Gene editing :For gene targeting, 1*10^6 K562 cells were collected and resuspended in 100ul Buffer R at a final density of 1.0 × 107 cells/mL， electroporated with 3 mg each of the ss ODN, 1.5mg gRNA and Cas9 (Addgene48138) by Neon Transfection System(Invitrogen) Transfected cells were plated onto the prepared 6 well plates. After transfection 48h, we use flow cytometry to isolate the single cell in 96 well plates. about 1 week later, we Identify the single cell clones by PCR and sanger sequence. The resistant colonies were picked and expanded until we generated the expected cell line. primers are listed in Supplemental.

Cell Cultures and differentiation--- K562 cells obtained from American Tissue Culture Collection. the cells of K562 and $K562^{-28(A>G)}$ were cultured in glutamine-minus RPMI 1640 medium(Gibco) with10% FBS in the presence of 1 mM sodium butyrate for 7 days to induce the erythroid differentiation, and then collected[39]. And the control cells were cultured in RPMI 1640 medium with 10% FBS and P/S antibiotics for 7 week at the same time.

Real-time Reverse transcriptase (RT)-PCR analysis----Total RNA was isolated from the cells by the TRIzol™ Reagent (invitrogen). Single stranded cDNA was synthesized with the oligo(dT) primer using PrimeScript™ RT reagent Kit with gDNA Eraser (Takara), the obtained cDNAs were analyzed by real-time PCR, using indicated primers. The *HBB* primers were 5'-GCTCGGTGCCTTTAGTGATG -3' (forward) and 5'-GCACACAGACCAGCACGTT -3' (reverse); for *HBG*, 5'-GGAAGATGCTGGAGGAGAAACC -3' (forward) and 5'-GTCAGCACCTTCTTGCCATGTG -3' (reverse). The cycling conditions were: 95℃ denaturation for 10 min, 95℃ for 15 s, annealing and extension at 60℃ for 40s, 40 cycles on the ABI step one machine.

Comparison the hemoglobin expression：

To comparison the hemoglobin expression of the uninduced cells （K562,K562$^{-28(A>G)}$, K562$^{-28(A>G)cor}$ dif ） and induced cells. K562dif K562$^{-28(A>G)}$ dif

we used Tetramethylbenzidine(TMB) Elisa Kit （Invitrogen） .10^5 cells from each of the test and control groups were resuspended in phosphate buffered saline (PBS) and mixed with equal volume of the Tetramethylbenzidine solution and then kept at room temperature for several mins. And then add double volume of Tetramethylbenzidine solution for stop solution. Brown-blue wells were regarded as positive and read at 450nm by Biotek epoch.Each treatment was performed in triplicate and each experiment was repeated for three times. Sample information in table1

Unstained/background			**Stained/test**		
K562	K562	K562	K562	K562	K562
K562$^{-28(A>G)}$	K562$^{-28(A>G)}$	K562$^{-28(A>G)}$	K562$^{-28(A>G)}$	K562$^{-28(A>G)}$	K562$^{-28(A>G)}$
K562$^{-28(A>G)cor}$	K562$^{-28(A>G)cor}$	K562$^{-28(A>G)cor}$	K562$^{-28(A>G)cor}$	K562$^{28(A>G)cor}$	K562$^{28(A>G)cor}$
K562-Dif	K562-Dif	K562-Dif	K562-Dif	K562-Dif	K562-Dif
K562$^{-28(A>G)}$ -	K562$^{-28(A>G)}$ –	K562$^{-28(A>G)}$ -	K562$^{-28(A>G)}$ -	K562$^{-28(A>G)}$ -	K562$^{-28(A>G)}$ –

Dif	Dif	Dif	Dif	Dif	Dif
$K562^{-28(A>G)cor}$ Dif	$K562^{-28(A>G)cor}$ Dif	$K562^{-28(A>G)cor}$ Dif	$K562^{-28(A>G)cor}$ Dif	$K562^{-28(A>G)cor}$ Dif	$K562^{-28(A>G)cor}$ Dif

Flow cytometry: We used CD235ab（Bio legend, USA）as the erythroid-specific surface marker which was determined by direct immunofluorescent staining with FITC-conjugated mouse monoclonal antibody. About 5 * 10^5 cells were harvested and counted, resuspended in 100ul PBS with Human BD Fc Block™(BD) for about 10mins at room temperature, then add100 ul FITC-conjugated with cd235ab diluted by 1:10 and incubated at 4 ℃ for 30 min. Cells were washed with ice-cold PBS three times and The fluorescence was measured assayed by flow cytometry of BD Aria III. Unstained group was used as antibody stain control for each samples (K562, K562-28, K562 induced, K562-28 induced)

RNA-Seq

RNA-Seq analysis

There are exceeding 2 million 100 bp pair-ended reads in each sample. Prior to assembly, Raw reads were filtered by SOAPnuke [40] with the parameters "-l 15 -q 0.2 -n 0.05". Reads were mapped to the human reference genome using HISAT2[41], which included both the genome sequences (GRCh38.p12) and known reference sequence (RefSeq) transcripts. Finally, the 80% of reads were aligned to human genome.

We used Samtools (Trapnell et al., 2012)[42] to sort and index the alignment files and Integrative Genomics Viewer (IGV) tool (Casero et al., 2015)[43] was used to visualize the reads. The sorted binary sequence analysis file (BAM files) was also used to generate UCSC Browser tracks with a genome

Coverage Bed from Bed Tools (Dennis et al., 2003)[44]. To this end, coverage files were normalized using the total signal for each sample.

The StringTie[45] suite of tools was used to calculate and compare gene expression levels and normalized as FPKMs (Fragments Per Kilobase of transcript per Million mapped reads). Differential expression analysis was assessed at each sample by comparing the pre- and post-induction cells using EdgeR Bioconductor package[46]. Differentially expressed Genes (DEGs) were identified when the $\log_2|\text{fold change}| > 1$ and the adjusted p-value < 0.01.

Gene ontology (GO) analysis

Gene ontology enrichment analysis of the gene sets was then performed on each sample using the cluster Profiler R package[47], including KEGG[48] pathways and Gene Ontology[49] (http://www.geneontology.org/), which were collected in Molecular Signatures Database (MSigDB)[50], Meanwhile, , DAVID (https://david.ncifcrf.gov/) and Metascape were utilized to assess the enrichment of functional categories (GO and KEGG) of the DEGs[51].

Transcription factor prediction

To compare the expression levels of transcription regulator genes between pre-induced and post-induced K562 cells, we collected a comprehensive transcription factor annotation from AnimalTFDB 3.0[52] and iRegulon[53],

and the results visualized using Cytoscape[54].

List of abbreviations

DMEM	Dulbecco's modified Eagle's medium
HBB	**Hemoglobin, Beta**

FCS	fetal calf serum
BSA	bovine serum albumin
assODN	asymmetric single strand oligo DNA nucleotides
$K562^{-28(A>G)}$	HBB-28(A>G) cell line
$K562^{-28(A>G)cor}$	Corrected HBB-28(G>A) cell line
Dif	Erythroid differentiation

Declarations

Competing interests

The authors declare that they have no competing interest.

FIGURE LEGEND

Figure 1. Generation of $K562^{-28\ (A>G)}$ cell line by CRISPR/Cas9 combined with asymmetric ssODN. (A) Experimental diagram of generation of the *HBB* -28 (A>G) mutation cell line in K562; (B) The region around *HBB* -28 are targeted with two asymmetric sgRNAs and ssODN are provided along with CRISPR/Cas9 DNA cleavage to generate *HBB* -28 (A>G) mutation. *sgRNA1* and *sgRNA2* are complementary to the sense and antisense strands respectively. Mutation site is indicated with red color in the middle of sequence. PAM: protospacer adjacent motif (orange); (C) Identification of the -28 (A>G) mutation by sanger sequencing. Expected mutation is shown in the red rectangle; (D) Expression of *HBB* mRNA determined by qPCR in $K562^{-28\ (A>G)}$ and K562; (E) Expression of *HBB* mRNA determined by ELASA with

494 benzidine staining in K562$^{-28\ (A>G)}$ and K562.

495 **Figure 2**. Transcriptome analysis of K562 and K562$^{-28\ (A>G)}$ cell lines before
496 erythrogenic differentiation. (A) Pairwise Pearson correlations are
497 represented in matrix between two K562 and two K562$^{-28\ (A>G)}$ samples before
498 differentiation ; (B) The correlation between representative K562$^{-28\ (A>G)}$ and
499 K562 sample before differentiation; (C) Heatmap shows the differentially
500 expressed genes (DEGs) between K562 and K562$^{-28\ (A>G)}$ cell lines; genes
501 related to hypoxia were showed on right (D) Enrichment analysis of GO ,
502 KEGG and Reactome pathways based on DEGs in K562$^{-28\ (A>G)}$ before
503 differentiation; (E) The predicted interaction map between transcription
504 factors (TF) in DEGs of K562$^{-28\ (A>G)}$ before differentiation; (F) The regulator
505 genes and their corresponsive target genes. The hypoxia gene were showed in
506 red.

507 **Figure 3**. Transcriptome analysis of co-regulated genes, including HBB genes,
508 in K562 and K562$^{-28\ (A>G)}$ cell lines after erythrogenic differentiation. (A)
509 Pairwise Pearson correlations are represented in matrix between isogenic cell
510 lines. The differentiated group are clustered together; (B) Heatmap shows the
511 co-regulated genes in K562 and K562$^{-28\ (A>G)}$ after erythrogenic differentiation
512 when compared to those before differentiation. (C) KEGG signaling pathways
513 enriched in differentiated K562 and K562$^{-28\ (A>G)}$ when compared to their
514 corresponding cell lines before differentiation; (D) The Integrative Genomics
515 Viewer (IGV) shows the *HBB* gene expression in K562 and K562$^{-28\ (A>G)}$ cell
516 lines; (E and F) Expression and change trends of globin genes determined by
517 RNA-seq in the K562 and K562$^{-28\ (A>G)}$ cell lines before and after induction;
518 (G and H) Expression and change trends of globin *HBB* and *HBG* determined
519 by qPCR in the K562 and K562$^{-28\ (A>G)}$ cell lines before and after induction;
520 (I) Expression of key transcription factors related to erythroid differentiation.

521 **Figure 4**. Transcriptome analysis of differentially expressed genes in K562
522 and K562$^{-28\ (A>G)}$ cell lines after erythrogenic differentiation. (A) Heatmap

shows DEGs in $K562^{-28\ (A>G)}$ when compared to K562 after differentiation; (B) Signaling pathways analysis based on DEGs of $K562^{-28\ (A>G)}$ compared to K562 after differentiation; (C) Reactome analysis of critical DEGs and their related KEGG pathways in differentiated $K562^{-28\ (A>G)}$ when compared to its corresponsive K562 control. (D) the prediction of TFs in K562 after differentiation. (E) the prediction of TFs in $K562^{-28\ (A>G)}$ after differentiation.

Figure 5. Genes and key pathways are reversed in mutation corrected $K562^{-28(A>G)cor}$ cell line. (A) the identify of HBB gene in $K562^{-28(A>G)cor}$ by sanger sequencing. (B) The correlations between the K562 and $K562^{-28(A>G)cor}$; (C) Heatmap shows the up-regulated and down-regulated DEGs in K562, $K562^{-28\ (A>G)}$ and $K562^{-28(A>G)cor}$; (D) Differentially regulated signaling pathways in $K562^{-28cor}$ when compared to $K562^{-28\ (A>G)}$; (E) the recovery of genes relative to Key pathway and hypoxia.

Reference

1. de Dreuzy E, Bhukhai K, Leboulch P, Payen E. **Current and future alternative therapies for beta-thalassemia major**. *Biomed J* 2016; 39(1):24-38.
2. Mansilla-Soto J, Riviere I, Boulad F, Sadelain M. **Cell and Gene Therapy for the Beta-Thalassemias: Advances and Prospects**. *Hum Gene Ther* 2016; 27(4):295-304.
3. Galanello R, Origa R. **Beta-thalassemia**. *Orphanet J Rare Dis* 2010; 5:11.
4. Origa R. **beta-Thalassemia**. *Genet Med* 2017; 19(6):609-619.
5. Weatherall DJ, Williams TN, Allen SJ, O'Donnell A. **The population genetics and dynamics of the thalassemias**. *Hematol Oncol Clin North Am* 2010; 24(6):1021-1031.
6. Cao A, Galanello R. **Beta-thalassemia**. *Genet Med* 2010; 12(2):61-76.
7. Liang P, Ding C, Sun H, Xie X, Xu Y, Zhang X, et al. **Correction of beta-thalassemia mutant by base editor in human embryos**. *Protein Cell* 2017; 8(11):811-822.
8. Kumar SR, Markusic DM, Biswas M, High KA, Herzog RW. **Clinical development of gene therapy: results and lessons from recent successes**. *Mol Ther Methods Clin Dev* 2016; 3:16034.
9. Xu P, Tong Y, Liu XZ, Wang TT, Cheng L, Wang BY, et al. **Both TALENs and CRISPR/Cas9 directly target the HBB IVS2-654 (C > T) mutation in beta-thalassemia-derived iPSCs**. *Sci Rep* 2015; 5:12065.
10. Lai K, Huang G, Su L, He Y. **The prevalence of thalassemia in mainland China: evidence from epidemiological surveys**. *Sci Rep* 2017; 7(1):920.
11. Orkin SH, Sexton JP, Cheng TC, Goff SC, Giardina PJ, Lee JI, et al. **ATA box transcription mutation in beta-thalassemia**. *Nucleic Acids Res* 1983; 11(14):4727-4734.
12. Taher AT, Weatherall DJ, Cappellini MD. **Thalassaemia**. *The Lancet* 2018; 391(10116):155-167.

13. Taghavifar F, Hamid M, Shariati G. **Gene expression in blood from an individual with beta-thalassemia: An RNA sequence analysis**. *Mol Genet Genomic Med* 2019; 7(7):e00740.
14. Men K, Duan X, He Z, Yang Y, Yao S, Wei Y. **CRISPR/Cas9-mediated correction of human genetic disease**. *Sci China Life Sci* 2017; 60(5):447-457.
15. Zhang X, Wang L, Liu M, Li D. **CRISPR/Cas9 system: a powerful technology for in vivo and ex vivo gene therapy**. *Sci China Life Sci* 2017; 60(5):468-475.
16. Niu X, He W, Song B, Ou Z, Fan D, Chen Y, et al. **Combining Single Strand Oligodeoxynucleotides and CRISPR/Cas9 to Correct Gene Mutations in beta-Thalassemia-induced Pluripotent Stem Cells**. *J Biol Chem* 2016; 291(32):16576-16585.
17. Paquet D, Kwart D, Chen A, Sproul A, Jacob S, Teo S, et al. **Efficient introduction of specific homozygous and heterozygous mutations using CRISPR/Cas9**. *Nature* 2016; 533(7601):125-129.
18. Jafari M, Ghadami E, Dadkhah T, Akhavan-Niaki H. **PI3k/AKT signaling pathway: Erythropoiesis and beyond**. *J Cell Physiol* 2019; 234(3):2373-2385.
19. Grass JA, Boyer ME, Pal S, Wu J, Weiss MJ, Bresnick EH. **GATA-1-dependent transcriptional repression of GATA-2 via disruption of positive autoregulation and domain-wide chromatin remodeling**. *Proc Natl Acad Sci U S A* 2003; 100(15):8811-8816.
20. Witt O, Sand K, Pekrun A. **Butyrate induced erythroid differentiation of human K562 cells involves inhibition of ERK and activation of p38 MAP kinase pathways**. 2000; 95(7):2391-2396.
21. Yang J, Kawai Y, Hanson RW, Arinze IJJJoBC. **Sodium Butyrate Induces Transcription from the Gα i2 Gene Promoter through Multiple Sp1 Sites in the Promoter and by Activating the MEK-ERK Signal Transduction Pathway ***. 2001; 276(28):25742.
22. Palstra RJ, de Laat W, Grosveld F. **Beta-globin regulation and long-range interactions**. *Advances in genetics* 2008; 61:107-142.
23. Stamatoyannopoulos G. **Control of globin gene expression during development and erythroid differentiation**. *Experimental Hematology* 2005; 33(3):259-271.
24. Wienert B, Martyn GE, Funnell APW, Quinlan KGR, Crossley M. **Wake-up Sleepy Gene: Reactivating Fetal Globin for beta-Hemoglobinopathies**. *Trends Genet* 2018; 34(12):927-940.
25. Zhou D, Liu K, Sun CW, Pawlik KM, Townes TM. **KLF1 regulates BCL11A expression and gamma- to beta-globin gene switching**. *Nat Genet* 2010; 42(9):742-744.
26. Bruchova-Votavova H, Yoon D, Prchal JTJL, Lymphoma. **MiR-451 enhances erythroid differentiation in K562 cells**. 2010; 51(4):686-693.
27. Qun HE, Yuan LBJCMJ. **Dopamine inhibits proliferation, induces differentiation and apoptosis of K562 leukaemia cells**. 2007; 120(011):970-974.
28. Park JI, Choi HS, Jeong JS, Han JY, Kim IHJCGD. **Involvement of p38 kinase in hydroxyurea-induced differentiation of K562 cells**. 2001; 12(9):481-486.
29. Li B, Ding L, Li W, Story MD, Pace BS. **Characterization of the transcriptome profiles related to globin gene switching during in vitro erythroid maturation**. *BMC Genomics* 2012; 13:153.
30. Sankaran VG, Xu J, Orkin SH. **Advances in the understanding of haemoglobin switching**. *British Journal of Haematology* 2010; 149(2):181-194.
31. Chen Z, Luo HY, Steinberg MH, Chui DH. **BCL11A represses HBG transcription in K562 cells**. *Blood Cells Mol Dis* 2009; 42(2):144-149.
32. Dewitt MA, Magis W, Bray NL, Wang T, Corn JEJSTM. **Selection-free genome editing of the sickle mutation in human adult hematopoietic stem/progenitor cells**. 2016; 8(360):360ra134-

360ra134.

33. Li J, Lai Y, Shi L. **BCL11A Down-Regulation Induces gamma-Globin in Human beta-Thalassemia Major Erythroid Cells**. *Hemoglobin* 2018; 42(4):225-230.

34. Traxler EA, Yao Y, Wang YD, Woodard KJ, Kurita R, Nakamura Y, et al. **A genome-editing strategy to treat beta-hemoglobinopathies that recapitulates a mutation associated with a benign genetic condition**. *Nat Med* 2016; 22(9):987-990.

35. Martyn GE, Wienert B, Yang L, Shah M, Norton LJ, Burdach J, et al. **Natural regulatory mutations elevate the fetal globin gene via disruption of BCL11A or ZBTB7A binding**. *Nat Genet* 2018; 50(4):498-503.

36. Masuda T, Wang X, Maeda M, Canver MC, Sher F, Funnell APW, et al. **Transcription factors LRF and BCL11A independently repress expression of fetal hemoglobin**. 2016; 351(6270):285-289.

37. Liu N, Hargreaves VV, Zhu Q, Kurland JV, Hong J, Kim W, et al. **Direct Promoter Repression by BCL11A Controls the Fetal to Adult Hemoglobin Switch**. *Cell* 2018; 173(2):430-442 e417.

38. Ran FA, Hsu PD, Wright J, Agarwala V, Scott DA, Zhang F. **Genome engineering using the CRISPR-Cas9 system**. *Nat Protoc* 2013; 8(11):2281-2308.

39. Shariati L, Modaress M, Khanahmad H, Hejazi Z, Tabatabaiefar MA, Salehi M, et al. **Comparison of different methods for erythroid differentiation in the K562 cell line**. *Biotechnol Lett* 2016; 38(8):1243-1250.

40. Chen Y, Chen Y, Shi C, Huang Z, Zhang Y, Li S, et al. **SOAPnuke: a MapReduce acceleration-supported software for integrated quality control and preprocessing of high-throughput sequencing data**. *Gigascience* 2017; 7(1):gix120.

41. Kim D, Langmead B, Salzberg SL. **HISAT: a fast spliced aligner with low memory requirements**. *Nature methods* 2015; 12(4):357.

42. Li H, Handsaker B, Wysoker A, Fennell T, Ruan J, Homer N, et al. **The sequence alignment/map format and SAMtools**. *Bioinformatics* 2009; 25(16):2078-2079.

43. Robinson JT, Thorvaldsdóttir H, Winckler W, Guttman M, Lander ES, Getz G, et al. **Integrative genomics viewer**. *Nature biotechnology* 2011; 29(1):24.

44. Quinlan AR, Hall IM. **BEDTools: a flexible suite of utilities for comparing genomic features**. *Bioinformatics* 2010; 26(6):841-842.

45. Pertea M, Pertea GM, Antonescu CM, Chang T-C, Mendell JT, Salzberg SL. **StringTie enables improved reconstruction of a transcriptome from RNA-seq reads**. *Nature biotechnology* 2015; 33(3):290.

46. Robinson MD, McCarthy DJ, Smyth GK. **edgeR: a Bioconductor package for differential expression analysis of digital gene expression data**. *Bioinformatics* 2010; 26(1):139-140.

47. Yu G, Wang L-G, Han Y, He Q-Y. **clusterProfiler: an R package for comparing biological themes among gene clusters**. *Omics: a journal of integrative biology* 2012; 16(5):284-287.

48. Kanehisa M, Goto S. **KEGG: kyoto encyclopedia of genes and genomes**. *Nucleic acids research* 2000; 28(1):27-30.

49. Ashburner M, Ball CA, Blake JA, Botstein D, Butler H, Cherry JM, et al. **Gene ontology: tool for the unification of biology**. *Nature genetics* 2000; 25(1):25.

50. Liberzon A, Subramanian A, Pinchback R, Thorvaldsdóttir H, Tamayo P, Mesirov JP. **Molecular signatures database (MSigDB) 3.0**. *Bioinformatics* 2011; 27(12):1739-1740.

51. Dennis G, Sherman BT, Hosack DA, Yang J, Gao W, Lane HC, et al. **DAVID: database for**

annotation, visualization, and integrated discovery. *Genome biology* 2003; 4(9):R60.

52. Hu H, Miao Y-R, Jia L-H, Yu Q-Y, Zhang Q, Guo A-Y. **AnimalTFDB 3.0: a comprehensive resource for annotation and prediction of animal transcription factors**. *Nucleic acids research* 2018; 47(D1):D33-D38.

53. Janky R, Verfaillie A, Imrichová H, Van de Sande B, Standaert L, Christiaens V, et al. **Naval, Potier D, et al: iRegulon: From a gene list to a gene regulatory network using large motif and track collections**. *PLoS Comput Biol*; 10.

54. Shannon P, Markiel A, Ozier O, Baliga NS, Wang JT, Ramage D, et al. **Cytoscape: a software environment for integrated models of biomolecular interaction networks**. *Genome Res* 2003; 13(11):2498-2504.

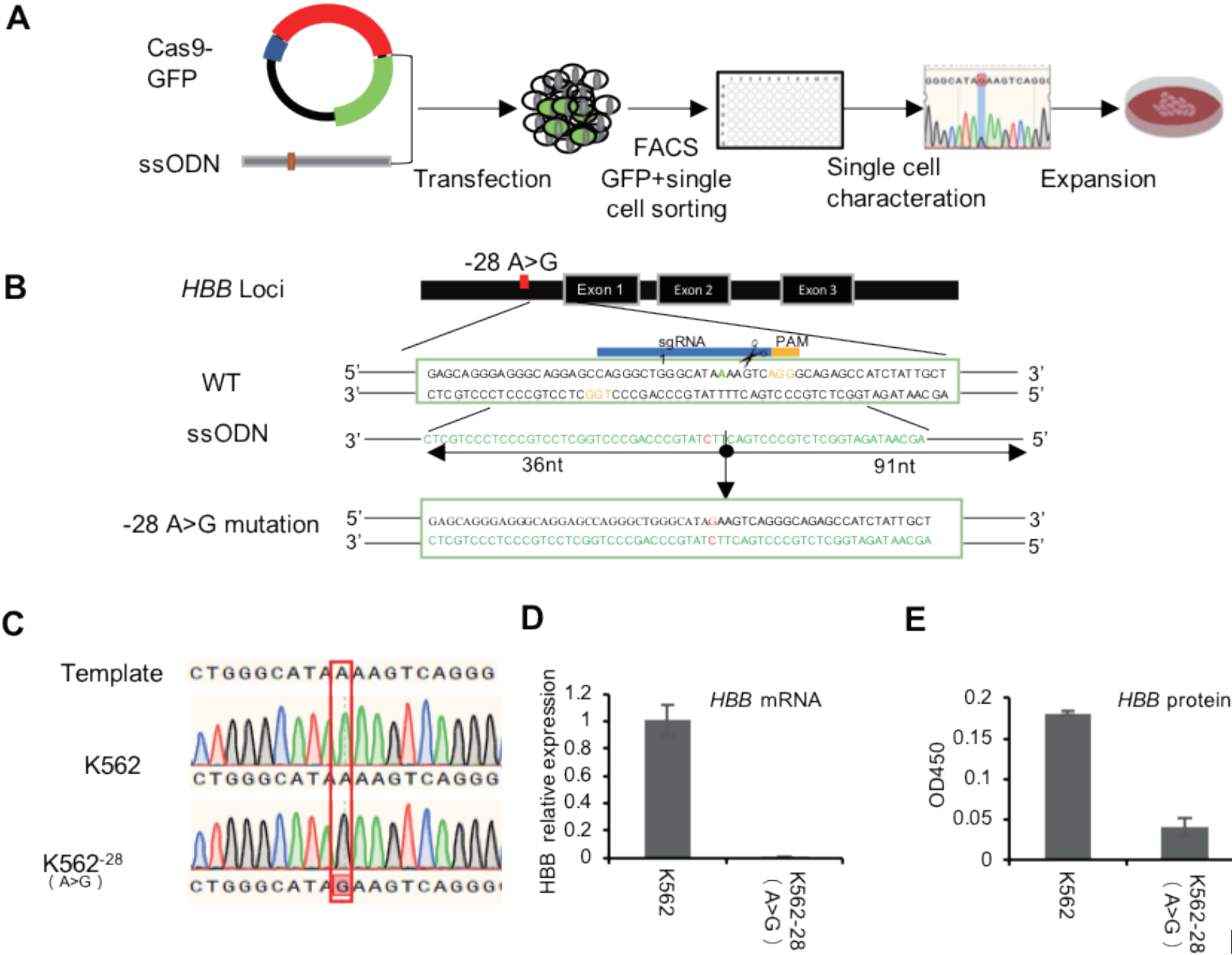
A
Cas9-
GFP
ssODN
Transfection
FACS
GFP+single
cell sorting
Single cell
characteration
Expansion
B
HBB Loci
-28 A>G
Exon 1
Exon 2
Exon 3
sgRNA
PAM
WT
ssODN
-28 A>G mutation
5'
3'
GAGCAGGGAGGGCAGGAGCCAGGGCTGGGCATAAAAGTCAGGGCAGAGCCATCTATTGCT
CTCGTCCCTCCCGTCCTCGGTCCCGACCCGTATTTTCAGTCCCGTCTCGGTAGATAACGA
CTCGTCCCTCCCGTCCTCGGTCCCGACCCGTATCTTCAGTCCCGTCTCGGTAGATAACGA
36nt
91nt
GAGCAGGGAGGGCAGGAGCCAGGGCTGGGCATAGAAGTCAGGGCAGAGCCATCTATTGCT
CTCGTCCCTCCCGTCCTCGGTCCCGACCCGTATCTTCAGTCCCGTCTCGGTAGATAACGA
C
Template
K562
K562-28
(A>G)
CTGGGCATAAAAGTCAGGG
CTGGGCATAGAAGTCAGGG
D
HBB relative expression
HBB mRNA
1.2
1
0.8
0.6
0.4
0.2
0
K562
K562-28
(A>G)
E
OD450
HBB protein
0.2
0.15
0.1
0.05
0
K562
K562-28
(A>G)

Figure 1

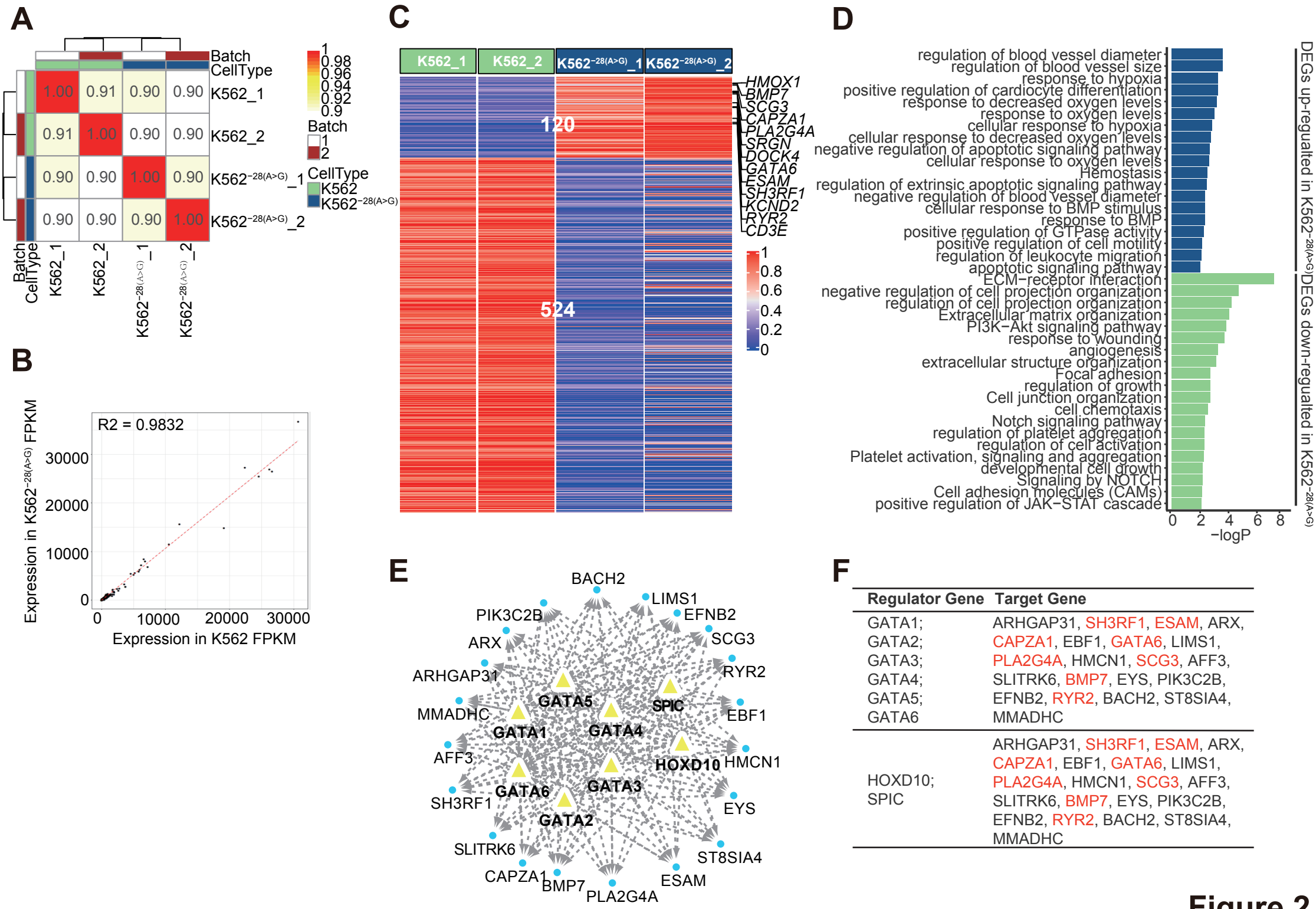

F

Regulator Gene	Target Gene
GATA1; GATA2; GATA3; GATA4; GATA5; GATA6	ARHGAP31, SH3RF1, ESAM, ARX, CAPZA1, EBF1, GATA6, LIMS1, PLA2G4A, HMCN1, SCG3, AFF3, SLITRK6, BMP7, EYS, PIK3C2B, EFNB2, RYR2, BACH2, ST8SIA4, MMADHC
HOXD10; SPIC	ARHGAP31, SH3RF1, ESAM, ARX, CAPZA1, EBF1, GATA6, LIMS1, PLA2G4A, HMCN1, SCG3, AFF3, SLITRK6, BMP7, EYS, PIK3C2B, EFNB2, RYR2, BACH2, ST8SIA4, MMADHC

Figure 2

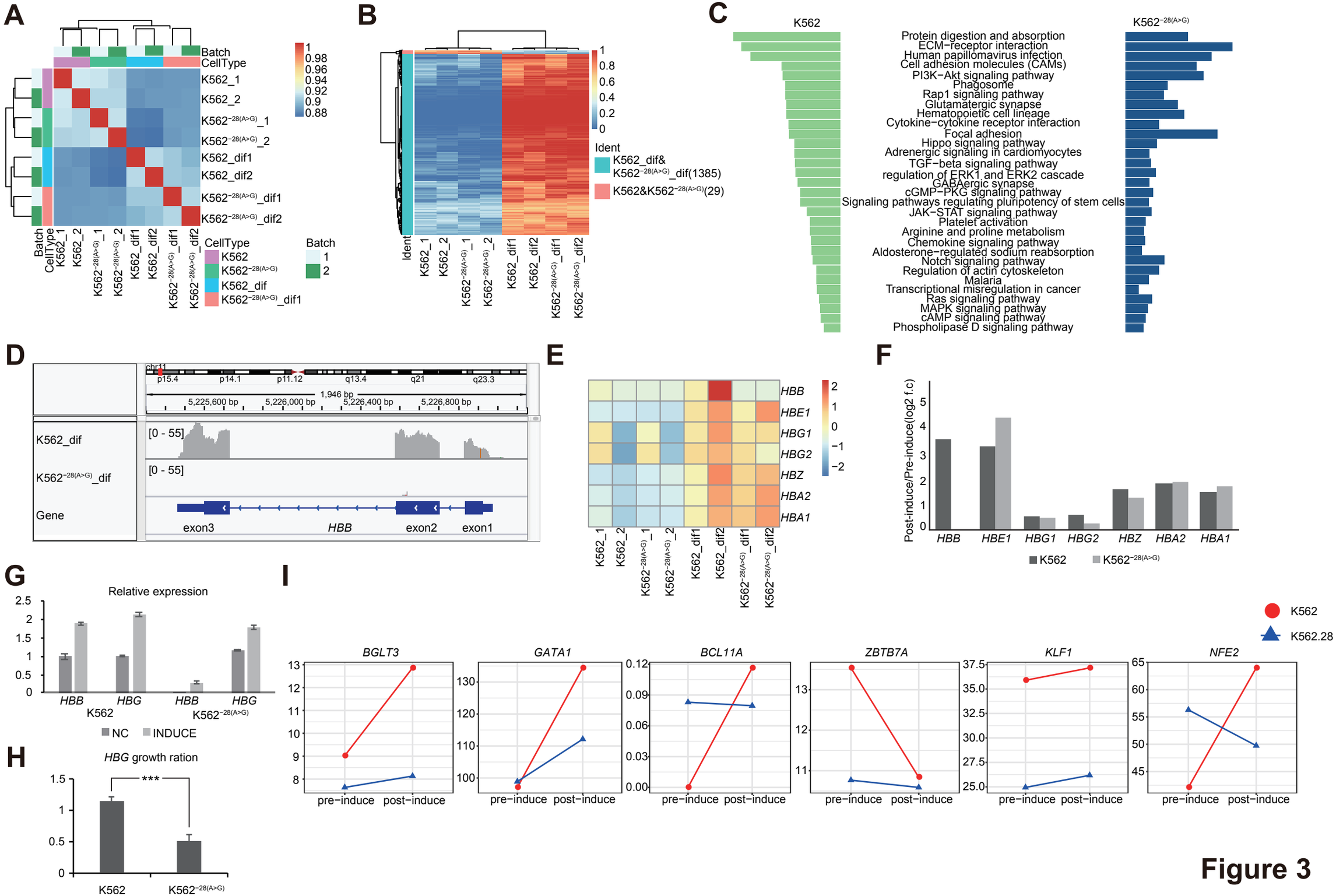
A
Batch
CellType
K562_1
K562_2
K562-28(A>G)_1
K562-28(A>G)_2
K562_dif1
K562_dif2
K562-28(A>G)_dif1
K562-28(A>G)_dif2
1
0.98
0.96
0.94
0.92
0.9
0.88
CellType
K562
K562-28(A>G)
K562_dif
K562-28(A>G)_dif1
Batch
1
2
B
Ident
K562_dif&
K562-28(A>G)_dif(1385)
K562&K562-28(A>G)(29)
1
0.8
0.6
0.4
0.2
0
C
K562
K562-28(A>G)
Protein digestion and absorption
ECM−receptor interaction
Human papillomavirus infection
Cell adhesion molecules (CAMs)
PI3K−Akt signaling pathway
Phagosome
Rap1 signaling pathway
Glutamatergic synapse
Hematopoietic cell lineage
Cytokine−cytokine receptor interaction
Focal adhesion
Hippo signaling pathway
Adrenergic signaling in cardiomyocytes
TGF−beta signaling pathway
regulation of ERK1 and ERK2 cascade
GABAergic synapse
cGMP−PKG signaling pathway
Signaling pathways regulating pluripotency of stem cells
JAK−STAT signaling pathway
Platelet activation
Arginine and proline metabolism
Chemokine signaling pathway
Aldosterone−regulated sodium reabsorption
Notch signaling pathway
Regulation of actin cytoskeleton
Malaria
Transcriptional misregulation in cancer
Ras signaling pathway
MAPK signaling pathway
cAMP signaling pathway
Phospholipase D signaling pathway
D
chr11
p15.4
p14.1
p11.12
q13.4
q21
q23.3
1,946 bp
5,225,600 bp
5,226,000 bp
5,226,400 bp
5,226,800 bp
K562_dif
[0 - 55]
K562-28(A>G)_dif
[0 - 55]
Gene
exon3
HBB
exon2
exon1
E
HBB
HBE1
HBG1
HBG2
HBZ
HBA2
HBA1
2
1
0
−1
−2
F
Post-induce/Pre-induce(log2 f.c)
HBB
HBE1
HBG1
HBG2
HBZ
HBA2
HBA1
K562
K562-28(A>G)
G
Relative expression
HBB
HBG
HBB
HBG
K562
K562-28(A>G)
NC
INDUCE
H
HBG growth ration
***
K562
K562-28(A>G)
I
K562
K562.28
BGLT3
GATA1
BCL11A
ZBTB7A
KLF1
NFE2
pre−induce
post−induce

Figure 3

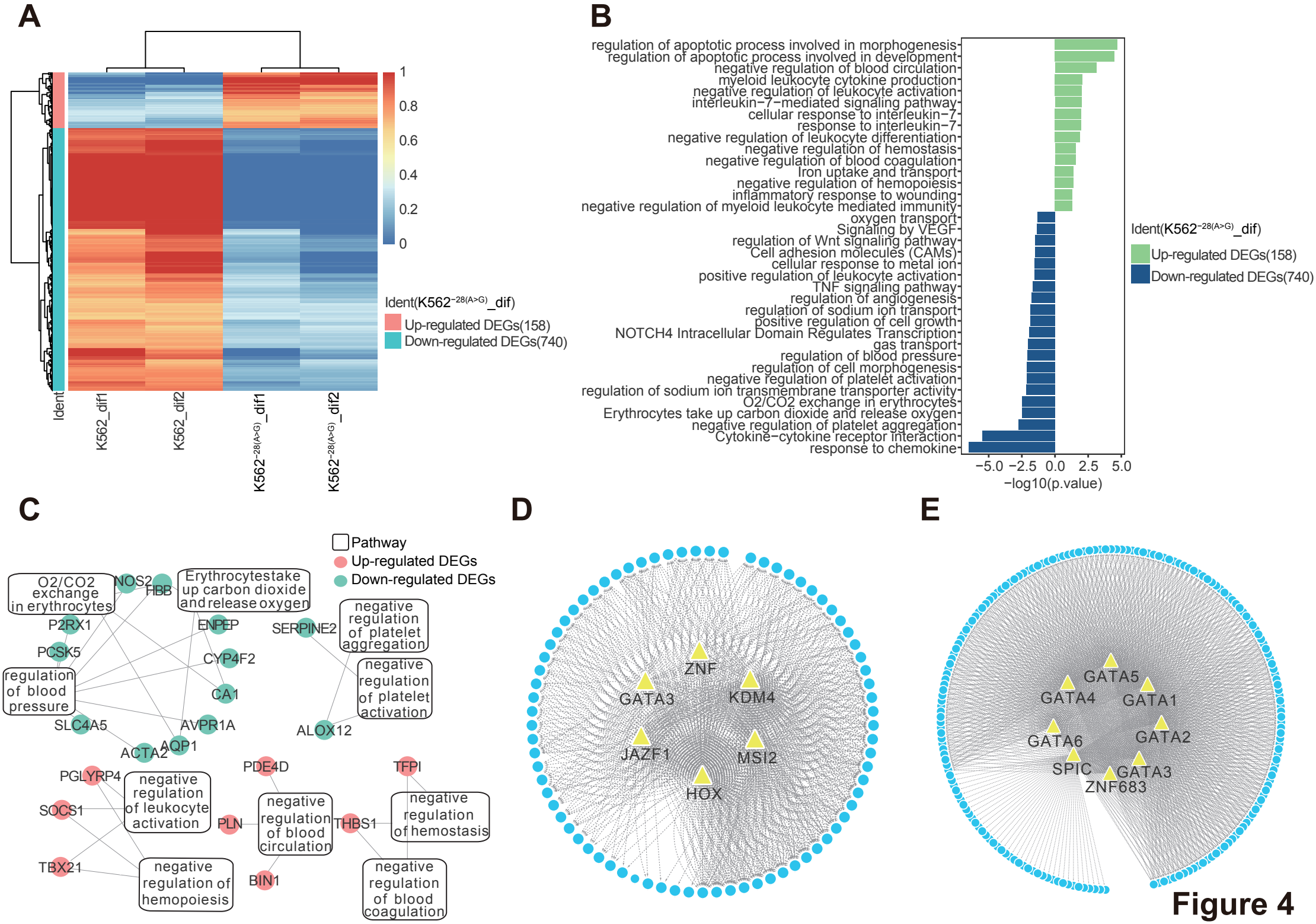
A
1
0.8
0.6
0.4
0.2
0
Ident(K562-28(A>G)_dif)
Up-regulated DEGs(158)
Down-regulated DEGs(740)
Ident
K562_dif1
K562_dif2
K562-28(A>G)_dif1
K562-28(A>G)_dif2
B
regulation of apoptotic process involved in morphogenesis
regulation of apoptotic process involved in development
negative regulation of blood circulation
myeloid leukocyte cytokine production
negative regulation of leukocyte activation
interleukin−7−mediated signaling pathway
cellular response to interleukin−7
response to interleukin−7
negative regulation of leukocyte differentiation
negative regulation of hemostasis
negative regulation of blood coagulation
Iron uptake and transport
negative regulation of hemopoiesis
inflammatory response to wounding
negative regulation of myeloid leukocyte mediated immunity
oxygen transport
Signaling by VEGF
regulation of Wnt signaling pathway
Cell adhesion molecules (CAMs)
cellular response to metal ion
positive regulation of leukocyte activation
TNF signaling pathway
regulation of angiogenesis
regulation of sodium ion transport
positive regulation of cell growth
NOTCH4 Intracellular Domain Regulates Transcription
gas transport
regulation of blood pressure
regulation of cell morphogenesis
negative regulation of platelet activation
regulation of sodium ion transmembrane transporter activity
O2/CO2 exchange in erythrocytes
Erythrocytes take up carbon dioxide and release oxygen
negative regulation of platelet aggregation
Cytokine−cytokine receptor interaction
response to chemokine
−5.0 −2.5 0.0 2.5 5.0
−log10(p.value)
Ident(K562-28(A>G)_dif)
Up-regulated DEGs(158)
Down-regulated DEGs(740)
C
Pathway
Up-regulated DEGs
Down-regulated DEGs
O2/CO2 exchange in erythrocytes
NOS2
HBB
Erythrocytestake up carbon dioxide and release oxygen
P2RX1
ENPEP
SERPINE2
negative regulation of platelet aggregation
PCSK5
CYP4F2
regulation of blood pressure
negative regulation of platelet activation
CA1
SLC4A5
AVPR1A
ALOX12
ACTA2
AQP1
PDE4D
TFPI
PGLYRP4
negative regulation of leukocyte activation
SOCS1
PLN
negative regulation of blood circulation
THBS1
negative regulation of hemostasis
TBX21
negative regulation of hemopoiesis
BIN1
negative regulation of blood coagulation
D
ZNF
GATA3
KDM4
JAZF1
MSI2
HOX
E
GATA5
GATA4
GATA1
GATA6
GATA2
SPIC
GATA3
ZNF683

Figure 4

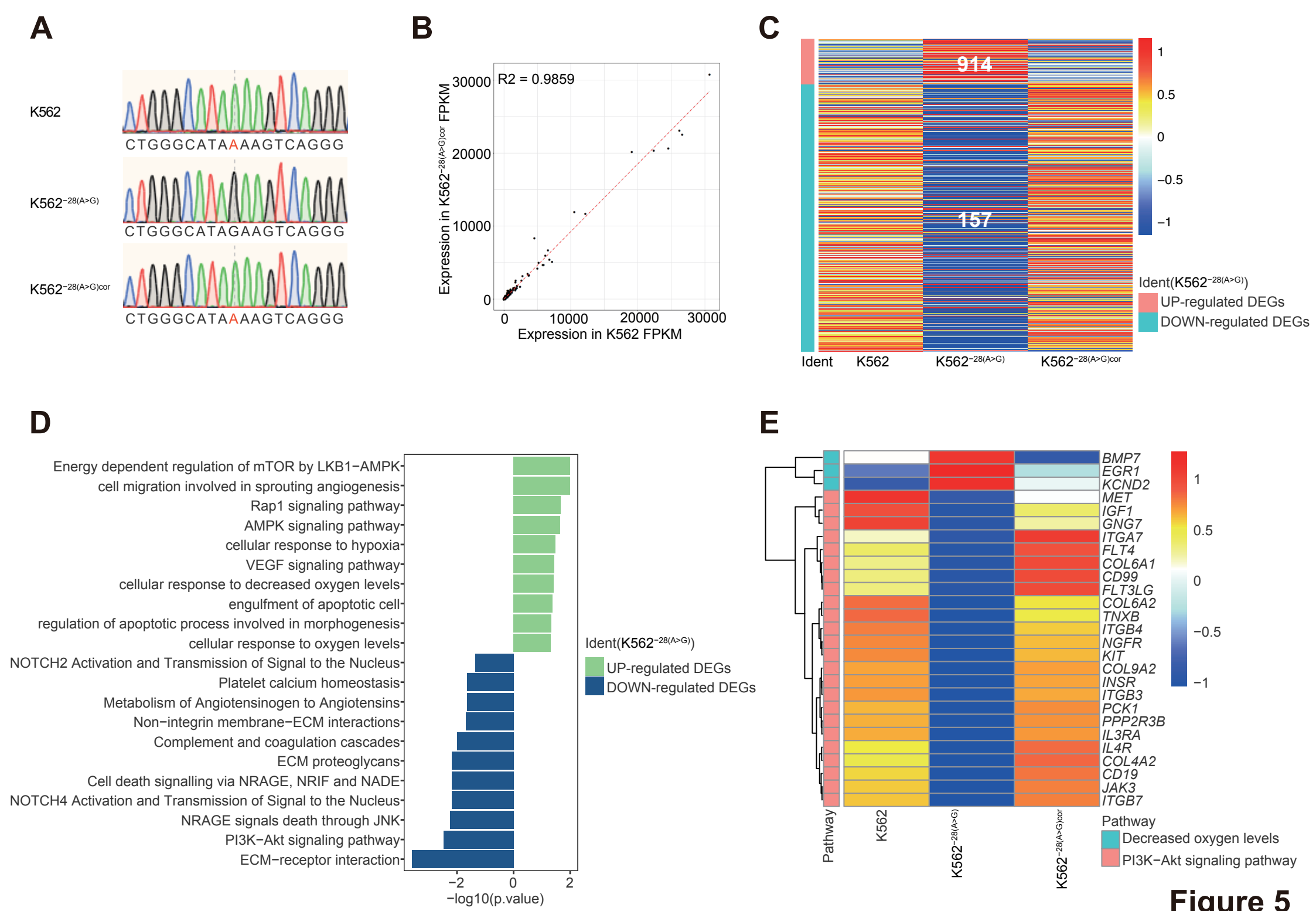
A
K562
CTGGGCATAAAAGTCAGGG
K562−28(A>G)
CTGGGCATAGAAGTCAGGG
K562−28(A>G)cor
CTGGGCATAAAAGTCAGGG
B
R2 = 0.9859
Expression in K562−28(A>G)cor FPKM
Expression in K562 FPKM
0
10000
20000
30000
C
914
157
1
0.5
0
−0.5
−1
Ident(K562−28(A>G))
UP-regulated DEGs
DOWN-regulated DEGs
Ident
K562
K562−28(A>G)
K562−28(A>G)cor
D
Energy dependent regulation of mTOR by LKB1−AMPK
cell migration involved in sprouting angiogenesis
Rap1 signaling pathway
AMPK signaling pathway
cellular response to hypoxia
VEGF signaling pathway
cellular response to decreased oxygen levels
engulfment of apoptotic cell
regulation of apoptotic process involved in morphogenesis
cellular response to oxygen levels
NOTCH2 Activation and Transmission of Signal to the Nucleus
Platelet calcium homeostasis
Metabolism of Angiotensinogen to Angiotensins
Non−integrin membrane−ECM interactions
Complement and coagulation cascades
ECM proteoglycans
Cell death signalling via NRAGE, NRIF and NADE
NOTCH4 Activation and Transmission of Signal to the Nucleus
NRAGE signals death through JNK
PI3K−Akt signaling pathway
ECM−receptor interaction
−2
0
2
−log10(p.value)
Ident(K562−28(A>G))
UP-regulated DEGs
DOWN-regulated DEGs
E
BMP7
EGR1
KCND2
MET
IGF1
GNG7
ITGA7
FLT4
COL6A1
CD99
FLT3LG
COL6A2
TNXB
ITGB4
NGFR
KIT
COL9A2
INSR
ITGB3
PCK1
PPP2R3B
IL3RA
IL4R
COL4A2
CD19
JAK3
ITGB7
1
0.5
0
−0.5
−1
Pathway
K562
K562−28(A>G)
K562−28(A>G)cor
Pathway
Decreased oxygen levels
PI3K−Akt signaling pathway

Figure 5